

Chaotic Dynamics in Coupled Microwave Oscillators

Rajeev J. Ram, Ralph Sporer, Hans-Richard Blank, and Robert A. York, *Senior Member, IEEE*

Abstract—This paper describes an investigation into possible chaotic behavior in a coupled-oscillator system and the possible control of this behavior for communications. The established mathematical models for these oscillator arrays are demonstrated to exhibit chaos when the coupling strength between oscillators is below the range for phase locking. The complexity and predictability of the array dynamics are analyzed by means of standard dynamical measures such as the Lyapunov exponents, the Kolmogorov–Sinai entropy, and the attractor dimension. We show that chaos in these oscillator arrays is low dimensional and well characterized; both necessary conditions for control and possible exploitation of chaos. Finally, the method of occasional proportional feedback is used to stabilize the output from the array while the array is still in the chaotic regime. Possible applications of these chaotic transmitters are also discussed.

I. INTRODUCTION

ARRAYS OF coupled nonlinear systems possess a rich catalog of potentially useful dynamics including mutual synchronization, which has been used to demonstrate novel beam-scanning techniques in microwave arrays [1] and mode locking. Coupled-oscillator systems have also been shown to reduce phase noise while increasing overall output power [2], [3]. Although it is not yet clear whether these effects will find practical use in microwave systems, the study of coupled-oscillators is also motivated by a broader role of synchronous behavior in many nonlinear biological systems, including cardiac and neural activity.

A clear understanding of coupled-oscillator systems requires a study of the full spectrum of operating regimes, including the nonsynchronous states. In recent years, the possibility of exploiting chaotic behavior of complex nonlinear systems has been raised. One intriguing possibility was proposed by Hayes, Grebogi, and Ott (HGO) [4]. In their proposal, a transmitter is separated into a chaotic power stage and a high-speed microelectronic control circuit. The free-running power stage is chaotic because of continuous “switching” between various unstable periodic orbits; an infinite number of unstable periodic states typically coexist with any chaotic state [5]. Since the chaotic state is arbitrarily close to any unstable periodic state,

a small control perturbation can cause the (normally chaotic) signal from the power stage to follow an “orbit” whose sequence represents the information to be communicated. Hayes *et al.* [6] have recently demonstrated this technique by controlling a 5-kHz chaotic oscillator circuit so that arbitrary bit sequences could be generated. With the HGO technique, there is no need for expensive high-speed electronics that are also capable of high power handling. The strict separation of the power stage and the high-speed electronics could allow for the fabrication of inexpensive high-speed wireless communication channels.

The major challenge for the HGO scheme is realization in a practical communication link. Coupled-oscillator arrays could present a suitable platform for chaotic communication systems. Modulation rates as high as 600 MHz have been demonstrated with oscillator arrays [7]. In this paper, we show that oscillator arrays have an accessible chaotic regime that exhibits low dimensionality, a necessary requirement for practical chaos control. In addition to the above-stated advantages of HGO channels, operation of the oscillator arrays in the chaotic regime may alleviate the bandwidth limits set by the intrinsic locking range of the arrays [8].

It is not difficult to observe chaos in single-oscillator systems. Van der Pol observed the appearance of irregular oscillations in an electrical circuit containing discharge tubes [9]. More recently, Fukushima and Yamada have replaced the discharge tube in Van der Pol’s apparatus with diode elements and have studied the dynamics of two such diode oscillators that were coupled by an inductive element [10]. We show in Section II that the dynamics of coupled-oscillator arrays are governed by a similar set of coupled Van der Pol equations.

Lasers are extensively studied nonlinear oscillators that exhibit chaos. Multimode lasers are examples of globally coupled oscillators [11] and laser arrays are examples of nearest neighbor coupled oscillators [12]. Again, the dynamics of laser arrays can be described by a set of modified Van der Pol equations. Control of chaos has thus far been demonstrated in a globally coupled oscillator system: an Nd:YAG multimode laser with an intracavity nonlinear crystal [13], [14].

Control and modulation of a chaotic system requires thorough characterization of the system dynamics. Despite the interest in oscillator arrays for synchronization or phase control, little consideration has been given to the dynamics of unsynchronized systems. In this paper, we obtain measures of the complexity and predictability of the array’s dynamics. To this end, the attractor dimension, the Kolmogorov–Sinai entropy, and the Lyapunov exponents are introduced and estimated. As a first step toward communications with chaotic antenna arrays, we employ the method of occasional proportional feedback (OPF) [15] to stabilize the output of an oscillator array while it is in the chaotic regime.

Manuscript received May 17, 1996. The work of R. J. Ram was supported by the National Science Foundation Center for Quantized Electronic Structures under the Vice-Chancellor’s Fellowship for Advanced Research in Quantum Structures, by the John and Fannie Hertz Foundation, and by the Army Research Office. The work of H.-R. Blank was supported by the Deutsche Forschungsgemeinschaft under a scholarship and by the Army Research Office. The work of R. Sporer was supported by Friedrich Alexander University of Erlangen, Germany, under a scholarship. The work of R. A. York was supported by the Army Research Office.

R. J. Ram, H.-R. Blank, and R. A. York are with the Department of Electrical and Computer Engineering, University of California at Santa Barbara, Santa Barbara, CA 93106 USA.

R. Sporer is with the Physikalisches Institut der Universität Erlangen-Nürnberg, D-91058 Erlangen, Germany.

Publisher Item Identifier S 0018-9480(00)09541-7.

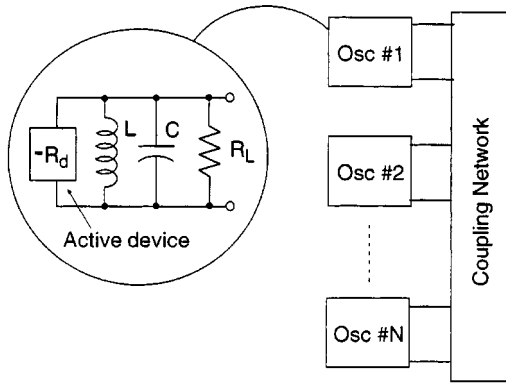


Fig. 1. Schematic diagram of coupled-oscillator system.

II. COUPLED-OSCILLATOR MODEL

To model these arrays, we choose a simple van der Pol model that applies generally to coupled oscillator systems while neglecting of the details of the coupling and the nonlinearity [16]. Such a simple theory has successfully modeled microwave oscillator experiments using Gunn, IMPATT, and MESFET devices [8], [17].

The Van der Pol equation [18] models the active device by a lumped negative resistance, which is embedded in a series resonant circuit (Fig. 1); any reactive component of the device impedance is considered part of the embedding network. The negative resistance R_d is assumed independent of frequency, but depends nonlinearly on the amplitude of oscillation. The circuit equation is

$$\frac{dV}{dt} + \omega_0^2 \int V dt + V \frac{\omega_0}{Q} \left[1 - \frac{R_d(|V|)}{R_L} \right] = \frac{\omega_0}{Q} V_{\text{inj}} \quad (1)$$

where R_L is the radiation resistance of the antennas, ω_0 is the resonant frequency of the circuit, V is the complex (phasor) output voltage, Q is the Q -factor of the embedding network, and V_{inj} represents any externally injected signals. The Q -factor is sufficiently high ($Q > 10$) so that the oscillator frequency will remain close to ω_0 and, therefore, the amplitude and phase terms will be slowly varying functions of time (compared with the period of oscillation). The output voltage can then be written as

$$V = A(t)e^{j(\omega_0 t + \phi(t))} = A(t)e^{j\theta(t)} \quad (2)$$

where A is the amplitude of oscillation, and θ is the instantaneous phase. Following Van der Pol [7], the device saturation is modeled by a quadratic such that

$$1 - R_d/R_L \simeq \mu(\alpha_0^2 - |V|^2) \quad (3)$$

where α_0 is the free-running amplitude of oscillation, and μ is an empirical nonlinearity parameter describing the oscillator. This weak quadratic nonlinearity is the simplest nonlinearity that approximates the behavior of a wide range of active devices. Using (2), the amplitude and phase dynamics can be written

separately as

$$\frac{dA}{dt} = \mu \frac{\omega_0}{2Q} A(\alpha_0^2 - A^2) + \frac{\omega_0}{2Q} A \text{Re} \left\{ \frac{V_{\text{inj}}}{V} \right\} \quad (4a)$$

$$\frac{d\theta}{dt} = \omega_0 + \frac{\omega_0}{2Q} \text{Im} \left\{ \frac{V_{\text{inj}}}{V} \right\} \quad (4b)$$

where $\text{Re}\{\}$ and $\text{Im}\{\}$ denote the real and imaginary parts of the bracketed expression, respectively.

For a system of coupled oscillators, the mutual interaction between oscillators i and j is described by a complex coupling coefficient κ_{ij} , which has a magnitude and phase given by

$$\kappa_{ij} \equiv \varepsilon_{ij} e^{-j\Phi_{ij}}. \quad (5)$$

In most arrays, reciprocity will hold so that $\kappa_{ij} = \kappa_{ji}$. This coupling parameter is unitless and defined such that in a system of N oscillators, the injected signal at the i th oscillator can be written as

$$V_{\text{inj}} = \sum_{j=1}^N \kappa_{ij} V_j \quad (6)$$

where V_i is the complex (phasor) output voltage of the i th oscillator. The system dynamics are described by

$$\frac{dV_i}{dt} = V_i \left[\frac{\mu\omega_i}{2Q} (\alpha_i^2 - |V_i|^2) + j\omega_i \right] + \frac{\omega_i}{2Q} \sum_{j=1}^N \kappa_{ij} V_j, \quad (7)$$

$$i = 1, 2, \dots, N$$

where the subscript i denotes the i th oscillator. For simplicity, it is assumed that all of the oscillators have approximately the same Q - and μ -factors. Writing $V_i = A_i e^{j\theta_i}$ enables the amplitude and phase dynamics to be separated as

$$\frac{dA_i}{dt} = \frac{\mu\omega_i}{2Q} (\alpha_i^2 - A_i^2) A_i + \frac{\omega_i}{2Q} \sum_{j=1}^N \varepsilon_{ij} A_j \cos(\Phi_{ij} + \theta_i - \theta_j) \quad (8a)$$

$$\frac{d\theta_i}{dt} = \omega_i - \frac{\omega_i}{2Q} \sum_{j=1}^N \varepsilon_{ij} \frac{A_j}{A_i} \sin(\Phi_{ij} + \theta_i - \theta_j), \quad (8b)$$

$$i = 1, 2, \dots, N.$$

When $\varepsilon_{ij} = 0$, the oscillators are uncoupled and (8) reduces to a set of independent sinusoidal oscillators with amplitudes $A_i = \alpha_i$ and frequencies ω_i .

In the limit of strong coupling between the oscillators, the amplitude dynamics can be significant. However, for exploring chaotic behavior, we are primarily interested in the case of weak coupling where the oscillators are unable to achieve a phase-locked state. In this limit, the amplitude variations are insignificant [19], and the dynamics are governed by the phase equations

$$\frac{d\theta_i}{dt} = \omega_i - \frac{\omega_i}{2Q} \sum_{j=1}^N \varepsilon_{ij} \frac{A_j}{A_i} \sin(\Phi_{ij} + \theta_i - \theta_j), \quad (9)$$

$$i = 1, 2, \dots, N.$$

Note also that one of the phase variables is arbitrary and can be set to zero; an N -oscillator system has only $M = N - 1$ degrees of freedom. The ability to predetermine the number of dynamic variables in the coupled oscillator systems makes this system an ideal candidate for chaos control.

III. NUMERICAL TIME SERIES

The power transmitted by the antenna array is the natural variable for monitoring chaos in the coupled oscillators. The far-field power is the communication signal and can be related to the parameters in (9) by a superposition of the field patterns for the individual antennas

$$P(t) = \frac{1}{2R_L} \sum_{i=1}^N |A_i e^{j\theta_i}|^2. \quad (10)$$

In addition to the far-field power, it is necessary that we monitor the signal locally for input to the control circuit. An obvious choice for the local variable is the real part of the impedance into the antenna array. Energy conservation requires the input impedance to be proportional to the radiated power plus any ohmic losses.

In addition, we must choose a system variable that can be manipulated by the control circuit. Virtually any of the static variables that appear in (9) are a valid choice for a control parameter, i.e., the intrinsic frequency of the oscillator, the coupling strength, or the phase of the coupling constant. In this paper, we use the coupling strength as the relevant control parameter. High-speed modulation of the coupling strength may be accomplished by introducing active elements in the coupling network of a transmission-line coupled-oscillator array. For example, integration of an FET into the coupling network would allow us to attenuate the coupling between neighboring elements simply by varying the gate bias.

In order to investigate the dynamics of the oscillator arrays, we solve the set of coupled van der Pol equations in the time domain. The time series for the radiated power, radiation spectrum, and “phase portrait” are shown in Fig. 2 for three values of the coupling strength. The time series is calculated for a four-oscillator array with an initial frequency distribution of (9.988, 9.996, 10.004, and 10.012 GHz); each oscillator has a $Q = 20$. The sampling time is $\tau_s = 5$ ns. The 10-GHz carrier frequency is not observable from this time series data. As the oscillator strength is reduced below the range for phase locking, the time series becomes significantly more complex. Fig. 3 shows the global dynamics of the array. It is a density plot of the numerical time series as a function of the coupling strength; the frequency of occurrence for a given derivative of the radiated power is indicated by brightness. Three distinct regions can be identified in this figure. Coupling strengths greater than $\epsilon = 0.064$ are the phase-locked regime. Below $\epsilon = 0.020$, the dynamics appear irregular.

The literature on quasi-optical arrays has been restricted to the range where the oscillators are mutually injection locked. Operation of the oscillator arrays in the locking range does not exploit the rich dynamics of this system. For example, arrays

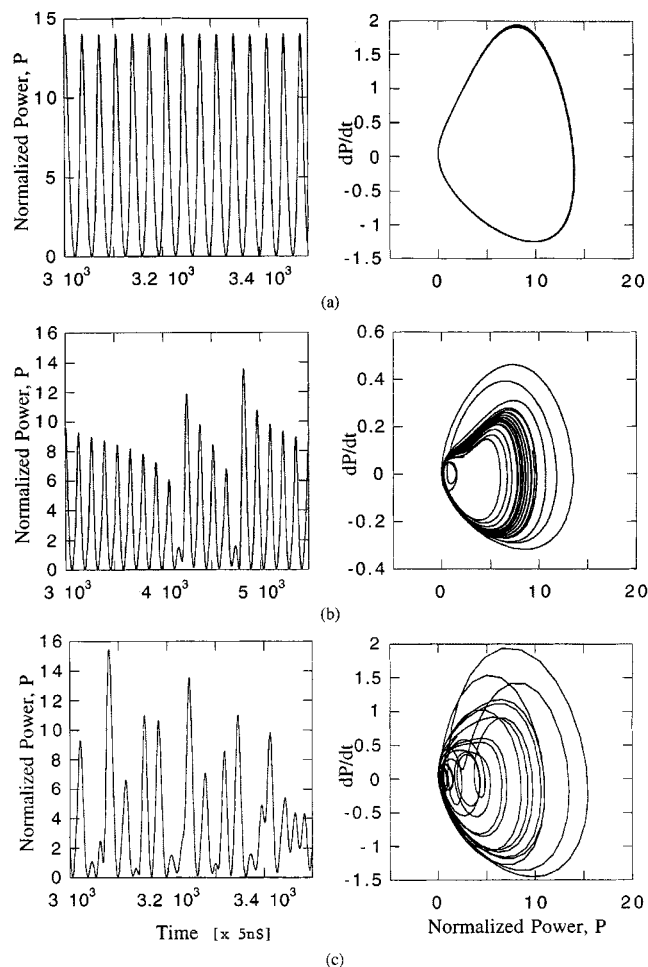


Fig. 2. Far-field power radiated by a four-element array. The power is plotted as a function of the time and as a function of its time derivative. Fig. 1(a)–(c) correspond to coupling strengths of 0.025, 0.020, and 0.015, respectively.

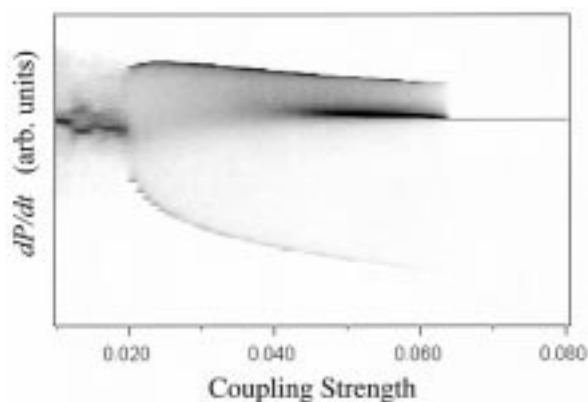


Fig. 3. Global dynamics of the four-element coupled-oscillator array. The frequency of occurrence for a given derivative of the radiated power is indicated by brightness. Three distinctly different operating regimes are visible. Coupling strengths greater than 0.064 result in phase locking of the oscillator elements. Coupling strengths below 0.020 result in chaotic fluctuations of the output power. Between chaos and phase locking is a continuous transition.

with oscillator strengths between $0.020 < \epsilon < 0.064$ exhibit periodic variations in the radiated power. Analysis of the power pattern shows that the beam from the array is scanning.

For intermediate coupling strengths, the arrays appear unstable and the power seems to fluctuate randomly. These fluctuations are entirely deterministic; there are no random variables or noise sources in the numerical simulations. The precision of the simulation is also not responsible for this instability. While reduction of the numerical precision from 16- to 8-bit alters the specific values of the time series, it does not affect its qualitative appearance. This seemingly random evolution of the radiated power is suggestive of chaos in the oscillator array.

There is a gradual transition between these two limits ($\epsilon = 0.020 - 0.064$). In the transition regime, the time series is quasi-periodic, but this periodicity is intermittently interrupted by large signal bursts. As the coupling strength is reduced toward the chaotic regime, the time between bursts becomes shorter until it is impossible to discern any clear periodicity. This appears to be an intermittency transition to chaos rather than the more familiar period-doubling route to chaos. Similar intermittency transitions to chaotic behavior have been observed in many systems, e.g., fluid transport, heat convection, and chemical reactions [20].

IV. CHARACTERIZING CHAOS

The best-known characteristic of a chaotic system is unpredictability, resulting from sensitivity to initial conditions (SIC). Even the slightest deviation from a given set of initial conditions yields a completely different output. Fig. 4 shows the time series for two arrays having the same coupling constants, but a slightly different initial phase distribution—one oscillator element has an additional 0.1° phase shift. Although the time series initially evolve together, after several time steps, the output from the two arrays appears to be completely independent.

Although SIC has come to be the hallmark of chaos, it is not unique to the chaotic regime. For example, a similar behavior can be observed in the intermittency transition regime where the time series is nearly periodic. Despite the apparent randomness, chaos refers to a specific well-defined type of dynamics. There are rigid constraints on the predictability and complexity of a chaotic system's evolution. Claims of chaos in many real systems have not been substantiated by rigorous analysis. Chaos in climate and brain-wave patterns has not been demonstrated; the analysis is limited by the large number of dynamical variables and poor data sets [21], [22].

A. Chaotic Attractors and Invariant Quantities

In this section, we discuss strategies for describing the dynamics of a system exhibiting such sensitivity to its starting values [23]. Although still useful, familiar techniques such as time- and frequency-domain analysis are often unable to reveal the patterns embedded within chaotic dynamics. It is necessary to investigate the dynamics of the system in a more abstract space called "phase space." Phase space is defined by a system's independent variables, e.g., the position and momentum of a linear damped harmonic oscillator or the relative phase differences in our coupled-oscillator arrays. The phase-space dimension is equal to the number of independent variables. Analysis of a power time series in phase space allows us to uncover the hidden structure in the behavior of the oscillator array.

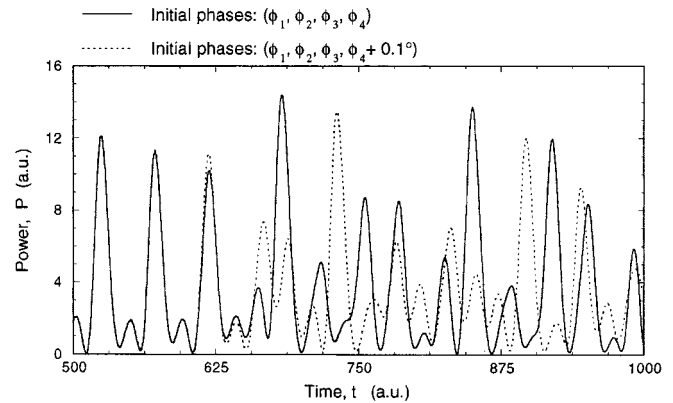


Fig. 4. Far-field power radiated by two identical four element arrays where one array has an additional 0.1° phase shift in an one-oscillator element.

In spite of SIC, all trajectories for a given set of control parameters converge to a single object in phase space: the attractor. The convergence of all trajectories to an attractor is guaranteed even if the control parameters are varied slightly. This characteristic behavior of a deterministic chaotic system is called structural stability. Small perturbations of the control parameter—e.g., from a feedback control circuit—do not change the attractor, they only change the trajectory in phase space. The structural stability of the attractor will be a necessary condition for chaos control of oscillator arrays. This invariance of the system dynamics occurs only when the control parameters are not close to any critical values. Near critical values of the control parameters, the system loses its structural stability and tends to undergo a transition to a different state; the attractor is then not defined. For example, the four-element array discussed in the previous section is not described by an attractor at the critical coupling constant $\epsilon 0.020$.

The set of Lyapunov exponents λ_i provides an intuitively appealing and yet powerful measure of SIC and dissipation, both of which are required for a chaotic system. The set of λ_i originates from a linear stability analysis. In this approximation, all solutions are of the form $\exp(\lambda_i t)$, $i = 1, \dots, M$, where M is the number of degrees of freedom, which—as mentioned before—is equal to the phase-space dimension. If one of the exponents is larger than zero, the distance between two initially nearby trajectories will increase exponentially with time in this direction; this exponential divergence is responsible for the SIC. If one of the λ_i is less than zero, the initial distance between two nearby trajectories will decrease exponentially with time. This negative Lyapunov exponent indicates the time scale for a perturbation to die out. It is a measure of the dissipation that allows a trajectory to be "pulled in" toward the attractor; without a negative exponent, an attractor could not exist. All dynamical systems that are drawn toward attractors¹ must also have one λ_i equal to zero, where this represents the direction of propagation where neighboring trajectories are parallel. A chaotic system has to have at least one positive, one negative, and one λ_i equal to zero.

¹This is true for all attractors, except point attractors, for which all Lyapunov exponents are negative.

In addition, the existence of the attractor allows a description of the system dynamics via other invariant quantities. One suitable quantity is the attractor dimension D_0 . The necessity for at least three different Lyapunov exponents for a chaotic system requires that the phase space in which the attractor is embedded be greater than three. Therefore, at least four oscillators (three relative phases) are required for the observation of chaos in the oscillator arrays represented by (9). In fact, the Poincaré–Bendixon theorem requires only that the attractor dimension of a chaotic system be larger than two. The attractor dimension for a chaotic system is typically fractional; this is an indication of the self-similarity of the phase-portrait.

Kolmogorov–Sinai entropy K_1 is a third important measure of the system dynamics. K_1 represents the rate at which information is “created” in the system. Consider a computer that tracks the state of dynamical systems and stores this information in a finite-size memory. Two initial states of a chaotic system that are indistinguishable due to the limited precision of the memory become distinguishable as the trajectories diverge due to SIC. Therefore, the amount of information needed to track a chaotic system is always increasing; K_1 is positive for a chaotic system. Two trajectories that start nearby remain nearby for a periodic system. Therefore, the amount of information needed to track the state of a periodic system does not change; K_1 is zero for a periodic system. For random evolution, two initially indistinguishable trajectories become distinguishable almost instantaneously; K_1 approaches infinity for random noise-driven systems. Our experience with various dynamical systems indicates that K_1 provides the most reliable indication of deterministic chaotic dynamics. Intuitively, the above discussion suggests that a large positive Lyapunov exponent results in a large K_1 entropy; it can be shown that $K_1 = \sum_{i=1}^{\infty} \lambda_i^+$, where the summation is only over the positive Lyapunov exponents.

The attractor dimension can also be estimated from the Lyapunov exponents. Kaplan and York conjectured that the attractor dimension

$$D_0 \geq j + \frac{1}{\lambda_{j+1}} \sum_{i=1}^j \lambda_i \quad (11)$$

where j is the positive integer for which the $\sum_{i=1}^j \lambda_i$ is still positive. This conjecture is a powerful method for estimating the attractor dimension.

All of the above quantities allow a characterization of deterministic chaotic systems via the analysis of corresponding attractors in phase space. While the dimension of an attractor gives an estimate of the number of the active degrees of freedom, the Kolmogorov–Sinai entropy and Lyapunov exponents indicate a time scale for which the oscillator array’s dynamics are predictable. A detailed analysis of experimental time series by the techniques mentioned above can aid in the construction of accurate theoretical models.

B. Characterizing Chaos in a Four-Element Array

In this section, we introduce techniques for the estimation of the Lyapunov exponents, attractor dimension, and entropy from numerical or experimental time series [24], [25]. Thus far, we have assumed that the evolution of all the systems independent

variables (i.e., the relative phases) could be monitored. While this is tenable for theoretical analysis, it is generally impossible to simultaneously measure the evolution of every independent variable. Often it is difficult to even determine the relevant degrees of freedom—which of the many parameters in an FET oscillator are relevant to the dynamics of the oscillator array? Also, it is, in general, not possible to calculate either the attractor dimension or the Kolmogorov–Sinai entropy from the time series; instead, we calculate the lower bounds for these measures. If we are to demonstrate chaos experimentally, we must first develop the necessary techniques with the numerical data.

Takens [26] demonstrated that, under certain limiting conditions, there is an equivalence of the true phase portrait with a reconstruction generated by a delay time embedding. In other words, a time delay reconstruction will not affect the actual values of D_0 , K_1 , or λ_i . The delay time method provides a phase portrait reconstruction even if the time series for only a single variable is known. In this case, we only observe the far-field power radiated by the array. The information contained in a measurement of all of the oscillator phases at a single time is reconstructed from a measurement of the radiated power $P(i)$ at many different times. In a d_E -dimensional embedding space, the vectors P_i are generated as follows:

$$P_i = \left(P(i), P(i + \tau), \dots, P(i + (d_E - 1)\tau) \right) \quad (12)$$

where τ is called the delay time. τ is arbitrary for an infinitely long and accurate time series, however, the choice of τ can be crucial for experimental or numerical data. In this paper, τ and d_E are varied, and the estimates for D_0 , K_1 , and λ_i are checked for stability.

As we mentioned earlier, even when the phase portrait has been constructed, we cannot, in general, determine D_0 from a given time series. D_0 is usually estimated by the correlation dimension D_2 , for which the relation $D_0 \geq D_2$ holds [27]. D_2 is relatively easy to compute and is widely used [28]. The calculation is performed by taking a reference point P_{ref} and measuring the distance to all other points P_j . The number of points within spheres of increasing radius r are counted. The mean over all reference points is called the correlation integral

$$C(r, d) = \sum_{i=1}^M \sum_{\substack{j=1 \\ j \neq i}}^M H(|P_i - P_j|) \quad (13)$$

where $H(|P_i - P_j|) = 1$ for $|P_i - P_j| \leq r$ and zero otherwise. The correlation integral is the average fraction of points within r . In a certain region, often referred to as the scaling region, $C(r, d_E)$ will follow a power law relation to r . The slope in that region

$$D_2 = \lim_{r \rightarrow 0} \frac{d \log C(r, d)}{d \log r} \quad (14)$$

is an estimate for the correlation dimension D_2 .

We have calculated the correlation integral $C(r, d_E)$ for 50 different radii r , following a logarithmic scaling to the maximal

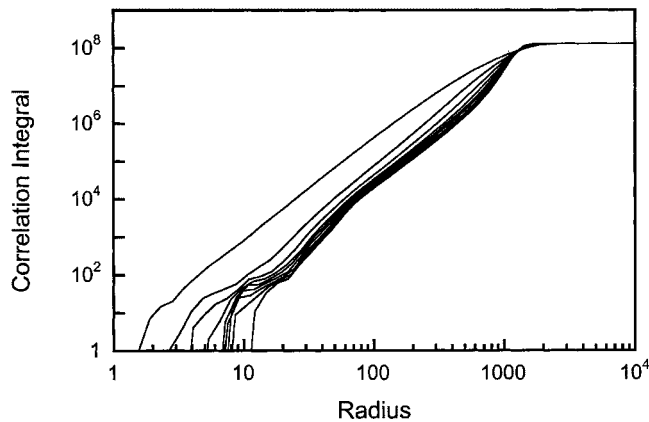


Fig. 5. Correlation integral for increasing hypersphere radii for embedding dimensions from $d_e = 2$ to 17. The correlation integrals coverage to a single curve as the embedding dimensions is increased.

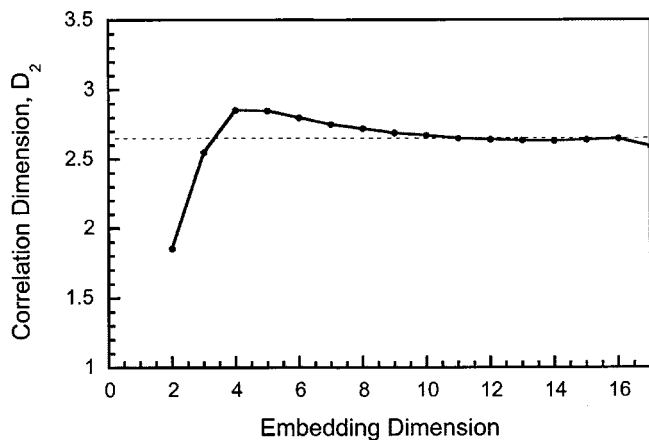


Fig. 6. Estimated dimension of the chaotic attractor for increasing embedding dimension.

extent of the attractor, as determined from the time series. The embedding dimension d_E was varied up to 25. We used a sample of 30 000 points for the calculation. The time delay τ was varied over a wide range. From $\tau = 5$ up to $\tau = 25$ (in units of sampling rate τ_s), the outcome remained qualitatively and quantitatively unchanged. We, therefore, fixed the value of $\tau = 10$ in the following. Furthermore, we excluded 200 neighbors of the reference point P_{ref} in order to avoid time correlations in the phase-space vectors, these spurious correlations frequently prevent the observation of the scaling region. Fig. 5 shows the correlation integral calculated from the power time series of the oscillator array with a coupling strength of $\epsilon = 0.015$.

The correlation integral shows the typical shape for a data set with finite length and precision, which result in the fluctuations of $C(r, d_E)$ at small radii ($r < 25$). In the range $25 < r < 600$, there is a well-defined scaling region where the slope of the curves follows the power law of (14) and the correlation dimension D_2 can be estimated. For radii larger than $r > 600$, the correlation integrals start to saturate, which corresponds to the coverage of the whole attractor by only a few hyperspheres. The correlation dimension converges to $D_2 = 2.63 \pm 0.03$, as shown in Fig. 6.

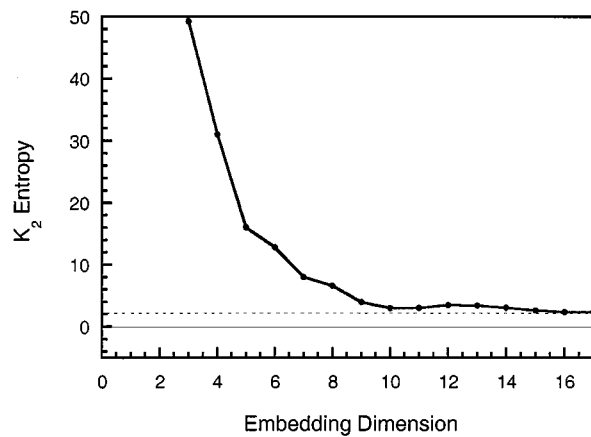


Fig. 7. Estimated Kolmogorov-Sinai entropy for increasing embedding dimension.

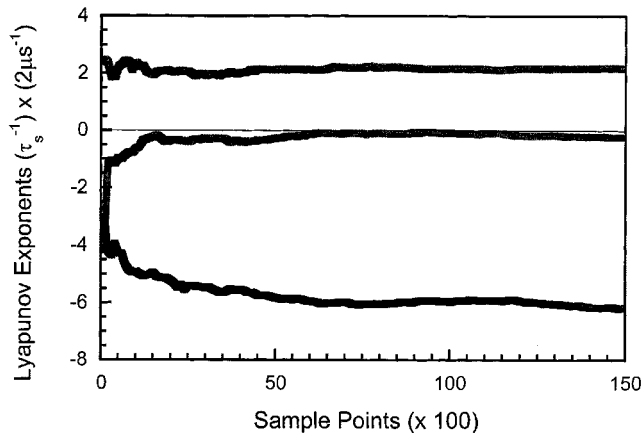


Fig. 8. Lyapunov λ_i exponents versus time for an embedding dimension of $d_E = 3$.

As with D_0 , it is hard to calculate K_1 directly from a finite time series. K_1 can be estimated from the K_2 entropy, where the relation $K_1 \geq K_2$ holds [29]. The K_2 entropy is related to the correlation integral through

$$K_2(r, d) = \frac{1}{\tau_s} \ln \left[\frac{C(r, d)}{C(r, d+1)} \right]$$

$$\lim_{\substack{r \rightarrow 0 \\ d \rightarrow \infty}} K_2(r, d) = K_2 \quad (15)$$

where τ_s denotes the sampling time. In order to obtain convergence for the calculation of the entropy by (15), it is usually necessary to rescale the distance for each dimension—a procedure outlined in detail in [30].

As shown in Fig. 7, a clear saturation is visible for the correlation entropy $K_2 = 2.04 \pm 0.17\tau_s^{-1}$. K_2 is well above zero, this provides a strong indication for a chaotic state.

A linear stability analysis can be used to extract the Lyapunov exponents from the constructed time series [31], [32]. Fig. 8 shows the Lyapunov exponents ($\lambda_1 = +2$, $\lambda_2 = 0$, and $\lambda_3 = -6 \tau_s^{-1}$) for an embedding dimension $d_E = 3$. The higher dimensions show a similar picture; for all embedding

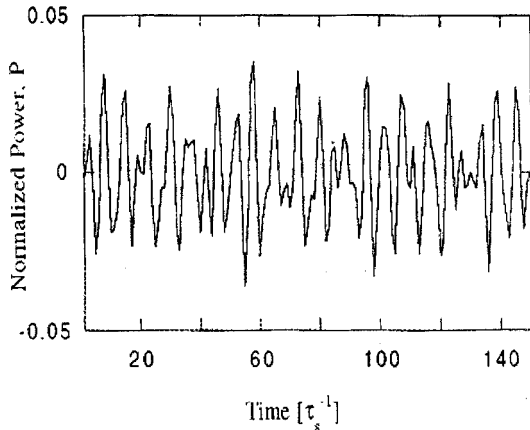


Fig. 9. Time series from an experimental array at 8 GHz.

dimensions, a positive Lyapunov exponent of $+2$ was found. Using the Kaplan–Yorke conjecture, the attractor dimension is estimated to be $D_0 = 2.35$ where $j = 2$ in (15).² This estimate is in agreement with the D_2 estimated from the correlation integral. In addition, the positive Lyapunov exponent is found to equal to the calculated K_2 entropy.

We want to stress that all of the methods described above must be used with extreme care. Note that all of the calculated quantities were stable with respect to changes in the embedding dimension; this check is necessary for the time-delay embedding procedure to be meaningful. There are additional restrictions arising from the influence of stationarity [24], metric in phase space [30], embedding parameters [33], [34], noise [35], [36], time correlations [37], and data length [38].

In summary, we have shown that the oscillator arrays exhibit several signatures of a chaotic system. Considering the underlying model and results of the preceding paragraph, we conclude that the coupled oscillator array shows low-dimensional chaotic behavior for a range of coupling strengths. Since K_2 was positive, the oscillator system is chaotic and it is assured that there are an infinite number of unstable periodic orbits that are accessible by small perturbations on the coupling strength. We have recently observed many of the complex time series discussed in this paper. The far-field power was measured in a coupled oscillator array with 8-GHz MESFET oscillator elements coupled to patch antennas [39]. An example is shown in Fig. 9.

V. CHAOS CONTROL

If we assign a symbol value to every periodic orbit, a chaotic symbol sequence is generated as the system switches between various orbits. Communication requires control of the symbol sequence, i.e., specifying the itinerary of orbits. In this section, we demonstrate control of the oscillator array by generating a regular symbol sequence. We employ a simple trial-and-error method where the parameters in the control algorithm are adjusted to obtain the desired periodic orbit. Stabilization of the system state is realized by the OPF algorithm [15].

The OPF algorithm samples the peak power $P_{\max}(i)$, and if it is within a given window, the coupling strength is modu-

² $d_E = 4$; $D_{KY} = 2.30$, $d_E = 5$, $D_{KY} = 2.37$, $d_E = 6$; $D_{KY} = 2.42$ or 2.66.

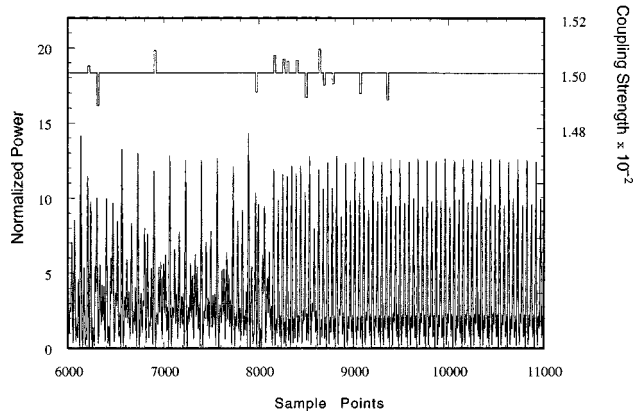


Fig. 10. Far-field power radiated by a four-element array with a coupling strength that is modulated so as to stabilize a periodic orbit. The instantaneous coupling strength is also shown.

lated proportionately to the difference between $P_{\max}(i)$ and the center of the window. If it is outside the window, no modulation is applied. The maximum correction is set to 1% of ϵ ; this ensures that the system is always described by a chaotic attractor. Scanning the center position of the windows selects different periodic orbits to be targeted.

Fig. 10 shows the time series for the radiated power and coupling strength for a four-oscillator array with $\epsilon = 0.015$. The control perturbation is applied for approximately 100 ns. A regular periodic orbit is stabilized by the control perturbations after approximately 10 000 time steps. Note that, for all values of the coupling strengths in Fig. 10, the free-running oscillator array was chaotic (see Fig. 3).

The complexity of the periodic orbit that is eventually stabilized is a result of the trial-and-error nature of the control algorithm. Careful analysis of the chaotic attractor can allow precise determination of the magnitude and frequency of the control pulse required to stabilize a periodic orbit. We chose the simple trial-and-error method since our goal is only to demonstrate that small ($<1\%$) perturbations of the coupling strength can stabilize the power radiated by the coupled oscillator array.

VI. CONCLUSIONS

In this paper, we have studied the dynamics of coupled nonlinear oscillators. We have shown that when the coupling strength between array elements is too small to allow phase locking, the antenna arrays exhibit low-dimensional chaos. Controlling the chaos in these arrays by small control perturbations indicates the potential of such oscillator arrays for chaotic communications. The combination of quasi-optical power combining and an external chaotic control may allow for high-power high-speed modulation in an inexpensive circuit.

Throughout this paper, we have used a simple model to describe the dynamics of coupled oscillator arrays. More accurate models tend to have the same underlying dynamics, but more degrees of freedom. The nonlinearity and coupling that we have employed are sufficiently general such that we can conclude that nearly all coupled oscillator arrays have similar chaotic operating regimes.

REFERENCES

- [1] J. J. Lynch, H. C. Chang, and R. A. York, "Coupled-oscillator arrays and scanning techniques," in *Active and Quasi-Optical Arrays for Solid-State Power Combining*, R. York and Z. Popović, Eds. New York: Wiley, 1997, ch. 4.
- [2] H.-C. Chang, X. Cao, U. Mishra, and R. A. York, "Phase noise in coupled oscillators: Theory and experiment," *IEEE Trans. Microwave Theory Tech.*, vol. 45, pp. 604–615, May 1997.
- [3] H.-C. Chang, X. Cao, M. J. Vaughan, U. K. Mishra, and R. A. York, "Phase noise in externally injection-locked oscillator arrays," *IEEE Trans. Microwave Theory Tech.*, vol. MTT-45, pp. 2035–2042, Nov. 1997.
- [4] S. Hayes, C. Grebogi, and E. Ott, "Communicating with chaos," *Phys. Rev. Lett.*, vol. 70, pp. 3031–3034, 1993.
- [5] T. Shinbrot, C. Grebogi, E. Ott, and J. A. Yorke, "Using small perturbations to control chaos," *Nature*, vol. 363, pp. 411–417, June 1993.
- [6] S. Hayes, C. Grebogi, E. Ott, and A. Mark, "Experimental control of chaos for communication," *Phys. Rev. Lett.*, vol. 73, pp. 1781–1784, Sept. 26, 1994.
- [7] R. A. York, "Nonlinear analysis of phase relationships in quasi-optical oscillator arrays," *IEEE Trans. Microwave Theory Tech. (Special Issue)*, vol. 41, pp. 1799–1809, Oct. 1993.
- [8] K. Kurokawa, "Injection-locking of solid-state microwave oscillators," *Proc. IEEE*, vol. 61, pp. 1386–1409, Oct. 1973.
- [9] V. Van der Pol and J. Van der Mark, "Frequency demultiplication," *Nature*, vol. 120, p. 363, 1927.
- [10] T. Yamada, K. Fukushima, and T. Yazaki, "Chaos in an electronic circuit—Experiment on coupled oscillator system," *Phase Trans.*, vol. 29, pp. 15–20, 1990.
- [11] C. Bracikowski and R. Roy, *Chaos*, vol. 1, p. 1749, 1991.
- [12] H. G. Winful and L. Rahman, "Synchronized and spatiotemporal chaos in arrays of coupled lasers," *Phys. Rev. Lett.*, vol. 65, pp. 1575–1578, 1990.
- [13] Z. Gills, C. Iwata, R. Roy, I. Schwarz, and I. Triandaf, "Tracking unstable steady states: Extending the stability regime of a multimode laser system," *Phys. Rev. Lett.*, vol. 69, pp. 3169–3172, 1992.
- [14] R. Roy, T. W. Murphy, T. D. Maier, and Z. Gills, "Dynamical control of a chaotic laser: Experimental stabilization of a globally coupled system," *Phys. Rev. Lett.*, vol. 68, pp. 1259–1262, Mar. 1992.
- [15] E. R. Hunt, "Stabilizing high-period orbits in a chaotic system: The diode resonator," *Phys. Rev. Lett.*, vol. 67, p. 1953, 1991.
- [16] K. D. Stephan, "Inter-injection locked oscillators for power combining and phased arrays," *IEEE Trans. Microwave Theory Tech.*, vol. MTT-34, pp. 1017–1025, Oct. 1986.
- [17] R. A. York and R. C. Compton, "Quasi-optical power-combining using mutually synchronized oscillator arrays," *IEEE Trans. Microwave Theory Tech.*, vol. 39, pp. 1000–1009, June 1991.
- [18] V. Van der Pol, "The nonlinear theory of electric oscillators," *Proc. IRE*, vol. 22, pp. 1051–1085, Sept. 1934.
- [19] N. Koppel, "Toward a theory of modeling central pattern generators," *Neural Control of Rhythmic Movements in Vertebrates*, 1988.
- [20] D. Ruelle and F. Takens, "On the nature of turbulence," *Commun. Math. Phys.*, vol. 20, pp. 167–192, 1971.
- [21] P. Grassberger, "Do climatic attractors exist?," *Nature*, vol. 323, pp. 609–612, 1986.
- [22] S. P. Layne, G. Mayer-Kress, and J. Holzfuss, "Problems associated with dimensional analysis of EEG data," in *Dimensions and Entropies in Chaotic Systems*, G. Mayer-Kress, Ed. Berlin, Germany: Springer-Verlag, 1986.
- [23] E. Ott, T. Sauer, and J. A. Yorke, Eds., *Coping with Chaos: Analysis of Chaotic Data and the Exploitation of Chaotic Systems*. New York: Wiley, 1995.
- [24] P. Grassberger, T. Schreiber, and C. Schaffrath, "Non-linear time sequence analysis," *Int. J. Bifurcation and Chaos*, Apr. 1991.
- [25] H.-R. Blank, Ph.D. dissertation, Friedrich Alexander Univ., Erlangen, Germany, 1994.
- [26] F. Takens, "Lecture notes in math," vol. 898, 1980.
- [27] C. W. Simm, M. L. Sawley, F. Skiff, and A. Pochelon, "On the analysis of experimental signals for evidence of deterministic chaos," *Helv. Phys. Acta*, vol. 60, pp. 510–551, 1987.
- [28] P. Grassberger and I. Procaccia, "Characterization of strange attractors," *Phys. Rev. Lett.*, vol. 50, p. 346, 1983.
- [29] ———, "Estimation of the Kolmogorov entropy from a chaotic signal," *Phys. Rev. Lett.*, vol. 50, p. 346, 1983.
- [30] M. Frank, H.-R. Blank, J. Heindl, M. Kaltenhauser, H. Kochner, W. Kreische, S. Poscher, R. Sporer, and T. Wagner, "Improvement of K_2 -entropy calculations by means of dimension scaled distances," *Phys. Rev. D. Part. Fields*, vol. 65, p. 359, 1993.
- [31] R. Stoop and P. F. Meier, "Evaluation of Lyapunov exponents and scaling functions from time series," *J. Opt. Soc. Amer. B, Opt. Phys.*, vol. 5, no. 5, p. 1037, 1988.
- [32] R. Stoop and J. Parisi, "Calculation of Lyapunov exponents avoiding spurious elements," *Phys. Rev. D, Part. Fields*, vol. 50, pp. 89–94, 1991.
- [33] J. W. Havstad and C. J. Ehlers, "Attractor dimensions of nonstationary dynamical systems from small datasets," *Phys. Rev. A, Gen. Phys.*, vol. 39, p. 845, 1989.
- [34] T. Buzug, T. Reimers, and G. Pfister, "Optimal reconstruction of strange attractors from purely geometrical arguments," *Europhys. Lett.*, vol. 13, p. 605, 1990.
- [35] J. Theiler, "Some comments on the correlation dimension of $1/f$ noise," *Phys. Lett. A*, vol. 155, p. 480, 1991.
- [36] T. Schreiber, "Extremely simple nonlinear noise reduction method," *Phys. Rev. E, Stat. Phys. Plasmas Fluids Relat. Interdiscip. Top.*, vol. 47, p. 2401, 1993.
- [37] J. Theiler, "Spurious dimension from correlation algorithms applied to limited time series data," *Phys. Rev. A*, vol. 34, p. 2427, 1986.
- [38] J.-P. Eckmann and D. Ruelle, "Fundamental limitations in estimating dimensions and Lyapunov exponents in dynamical systems," *Phys. Rev. D, Part. Fields*, vol. 56, p. 185, 1992.
- [39] R. J. Ram, R. Sporer, H.-R. Blank, P. Maccarini, H.-C. Chang, and R. A. York, "Chaos in microwave antenna arrays," in *IEEE Int. Microwave Symp. Dig.*, 1996, pp. 1875–1878.

Rajeev J. Ram received the B.S. degree in applied physics from the California Institute of Technology, Pasadena, in 1991, and the Ph.D. degree in electrical engineering from the University of California at Santa Barbara, in 1997.

He is currently an Associate Professor of electrical engineering and computer science at the Massachusetts Institute of Technology, Cambridge. He has spent the last ten years studying various aspects of electron and photon dynamics in semiconductors, including work on semiconductor lasers, microwave and optical transmission, quantum coherence, and thermodynamics of mesoscopic systems.

Ralph Sporer, photograph and biography not available at time of publication.

Hans-Richard Blank, photograph and biography not available at time of publication.



Robert A. York (S'85–M'89–SM'99) received the B.S. degree in electrical engineering from the University of New Hampshire, Durham, in 1987, and the M.S. and Ph.D. degrees in electrical engineering from Cornell University, Ithaca, NY, in 1989 and 1991, respectively.

He is currently a Professor of electrical and computer engineering at the University of California at Santa Barbara (UCSB), where his group is involved with the design and fabrication of novel microwave and millimeter-wave circuits and systems.

Dr. York was the recipient of the 1993 Army Research Office Young Investigator Award and the 1996 Office of Naval Research Young Investigator Award.